International Journal of Bifurcation and Chaos, Vol. 3, No. 6 (1993) 1363–1409

FROM CHAOS TO ORDER — PERSPECTIVES AND METHODOLOGIES IN CONTROLLING CHAOTIC NONLINEAR DYNAMICAL SYSTEMS

GUANRONG CHEN and XIAONING DONG
Department of Electrical Engineering, University of Houston, Houston, TX 77204-4793, USA

Received April 30, 1993

Controlling (or ordering) chaos is a new concept, which has recently drawn much attention from the communities of engineering, physics, chemistry, biomedical sciences and mathematics. This paper offers an overview of the different interpretations and approaches in the investigation of controlling chaos for various nonlinear dynamical systems. Relevant historical background is provided, several successful techniques are described and analyzed with necessary verifications, and some realistic yet instructive examples are included. The paper also aims at promoting more efforts to be devoted to this challenging and promising new direction of research, as well as its potential applications in nonlinear systems science and engineering.

1. Introduction

It has long been realized that most nonlinear dynamical systems do not follow simple, regular, and predictable trajectories, but swirl around in a randomlike and seemingly irregular, yet well-defined, fashion. As long as the process involved is nonlinear, even a very simple deterministic model may develop such complex behavior, which has now been understood and well accepted as *chaos* and has led to the dramatic development in nonlinear dynamical systems theory and engineering.

In the research areas of nonlinear dynamics, the topic that is concerned with controlling or ordering chaos has received ever increasing attention in the last few years. This is perhaps no surprise — it has always been human beings' aim and motivation to capture the laws which govern the abundance of such natural phenomena and to introduce order into it.

There certainly are good practical reasons for controlling or ordering chaos. First of all, "oscillations with little information content, or sudden unpredictable excursions of physical variables, are seldom likely to be desirable" [Mees, 1986]. Secondly, some chaos could lead systems to troubled or even catastrophic situations. For example, the chaoticity of particle dynamics is the cause of an enhanced diffusion across the confining magnetic field [Moon, 1987]. For a distributed artificial intelligence system, which is usually characterized by a massive collection of decision-making agents, the fact that an agent's decision also depends on those made by other agents leads to extreme complexity and nonlinearity of the overall system. More often than not, the information received by the agents about the "state" of the system may be "tainted," in the sense of being deterministic but unpredictable. When the system is loaded with imperfect information, agents of the system tend to make poor decisions concerning the choice of an optimal problem-solving strategy or cooperation with other agents. This would result in certain chaotic behavior of the agents and hence downgrade the performance of the entire system [Hogg & Huberman, 1991]. The reader is referred to Moon [1987] for more examples where chaos may have harmful consequences. Naturally, chaos should be reduced as much as possible, or totally eliminated, in these situations. Many engineering designs seek to avoid or eliminate the nonlinearity of the system and therefore the chaos, but usually at the expense of radically modifying the original system. If a physical system can be satisfactorily described by a

nonlinear mathematical model, then by exploring the model's parameter space, analytically or numerically, it is possible to know how chaos can be avoided by adjusting only a few key parameters, and the system can be designed accordingly. However, if the system is required to operate in a particular region of the parameter space, in which chaos is inevitable, or if it is very difficult, if not impossible, to access the system's internal parameters (e.g., in VLSI circuits), then one has to find some other ways to freeze out chaotic responses. Many possibilities have been suggested to achieve this.

Ironically, recent research shows that chaos may actually be useful under certain circumstances, and there has been a growing interest in meaningful utilization of the richness of chaos [Carrol & Pecora, 1991; Corcoran 1991; Freeman 1991; Pecora & Carroll, 1991]. Ott, Grebogi & Yorke [1990], for example, made an important observation that a chaotic attractor is actually composed of an extremely dense set of unstable limit cycles. If any of these limit cycles can be stabilized, one may desire to stabilize the one that characterizes certain maximal system performance. The key is that, in the situation where the system is meant for multiple purposes, one may only need to switch among different limit cycles in order for the operation of the system to achieve these different goals. If, on the other hand, the attractor is not chaotic, then changing the original system configuration may be necessary to accommodate different purposes. Thus, declared Ott *et al.*, "when designing a system intended for multiple uses, purposely building chaotic dynamics into the system may allow for the desired flexibilities" [Ott *et al.*, 1990].

Controlling chaos can sometimes be understood as a process of stabilizing unstable periodic orbits (limit cycles) in a chaotic system. Could the controlled biological chaos have anything to do with the way a human brain executes its task? For years, scientists have been trying to unravel why our brains endow us with inference, thought, recollection, reasoning and, most fascinating of all, laughter and tears. It has been discovered that the interactions among billions of nerve cells (neurons) and support cells in our brains are in fact chemically stimulated and controlled — chemicals called neurotransmitters travel across the synapse to trigger chemical activity of the neuron on the other side. Not enough of one neurotransmitter or too much of another could change our thinking, our mood, and even our muscle strength. Still, the mysteries about our brains are not fully disclosed. Yet, from another perspective, there are suggestions that "the controlled chaos of the brain is more than an accidental by-product of the brain complexity, including its myriad connections" and that "it may be the chief property that makes the brain different from an artificial-intelligence machine" [Freeman, 1991].

Whether the purpose is to reduce "bad" chaos or to induce the "good" variety, researchers in academic and scientific as well as industrial communities have felt strongly the necessity for systematic research on the topic of controlling chaos, and hence have proposed and experimented with various control schemes and applications, which may have indicated that the study of nonlinear systems dynamics and control has moved into a new era. It is just remarkable to see that, at long last, researchers from such diverse scientific and engineering backgrounds are joining together and aiming at one central theme — bringing order to chaos. The time has come to take an overview of the many different approaches and techniques developed in the last few years for controlling (or ordering) chaos.

While trying to avoid being an indifferent compilation of all the results available to the present authors, this paper attempts to provide the reader with pertinent and objective points of view on controlling chaos in an open and impartial manner. We have taken the liberty to comment on the intentions behind certain efforts, to evaluate the implications of the methods and results, and to speculate about generalizations or applications, if not to predict outright possible ongoing or future developments in this new research direction of nonlinear dynamics and control.

The presentations given in the following sections are not intended to be exhaustive, considering the ubiquity of chaos in nonlinear dynamical systems and considering the large, yet still growing, volume of related literature available on the topics under survey. The paper is essentially concerned with various perspectives and methodologies, namely: basic ideas, methods, techniques, and possible applications. We only include those approaches which allow us to illustrate what we believe to be their most telling features. Among the presentations that follow, some are fairly detailed accounts of every relevant aspect of the materials involved; some are merely "snapshots," where emphasis is placed upon the idea and the procedure of the control methods rather than their quantitative analysis. In addition, many of the discussions in

this article will be carried out within the context of a particular practical system or mathematical model. In order to gain a better understanding of the particular methods that interest the individual reader most, references to the original papers and many of the others cited therein should often be helpful.

Our survey begins with parametric variation methods in the next section, which have attracted much attention from a number of research groups. Section 3 is devoted to another successful method, the entrainment-migration controls, which may actually be considered as an open-loop control approach. In Sec. 4, the problem of controlling chaos is approached by virtue of conventional engineering controls. Section 5 presents several interesting related topics: the control of chaos in distributed artificial intelligence systems, a neural network approach, and a signal encoding method in a chaotic environment. Some researchers are already well on their way to utilizing the unique properties of chaos; one such example in using chaotic signals to synchronize dynamical systems is also reviewed in Sec. 5. The last section summarizes the control methods reviewed, serving the purpose of motivating and stimulating new efforts devoted to this challenging and promising direction of research.

2. Parametric Variation Methods

2.1. *An earlier attempt*

The idea of varying certain system parameter(s) to control chaos may be traced back to Pettini's paper of 1988 [Pettini, 1988], where he pointed out that a suitable relative variation of parameter may be able to reduce or suppress chaos. His suggestion was based on two observations: (i) parametric excitation can stabilize unstable fixed points of linear or linearized systems, and vice versa; (ii) the Jacobi equation for geodesic variations is a linear equation whose stable and unstable solutions correspond to regular and chaotic motions. The relative parameter variation he used was time-dependent, in the form $p \to p[1 + \eta f_p(t)]$, where η is a constant and $f_p(t) = f_p(t + T)$ for some $T > 0$. Pettini provided an example to show that chaos can indeed be reduced or eliminated in a dissipative system by means of parametric variation, where he considered the Duffing–Holmes oscillator modeled by

$$\ddot{x} + p_1\dot{x} - x + px^3 = q\cos\omega t\,, \qquad (1)$$

in which p_1, p, q, and ω are certain constants. This equation is a special case of the more general formulation of the Duffing equation

$$\ddot{x} + p_1\dot{x} + p_2 x + px^3 = q\cos\omega t\,, \qquad (2)$$

named after the mathematician who first studied it [Duffing, 1918]. This equation can be used to describe the hardening spring effect observed in many mechanical systems. Since its inception more than seven decades ago, it has emerged as one of the most important paradigms for the study of chaos, like the well-known van del Pol and Lorenz systems. The Duffing–Holmes equation can be used to describe the dynamics of a buckled beam, which is set in a nonuniform field of two fixed permanent magnets (when only one mode of vibration was considered). Pettini reformulated Eq. (1) in the form of $\dot{\mathbf{x}} = F_0(\mathbf{x}) + \epsilon F_1(\mathbf{x}, t)$ for some $\epsilon > 0$, namely:

$$\begin{bmatrix}\dot{x}\\ \dot{y}\end{bmatrix} = \begin{bmatrix} y \\ x - px^3\end{bmatrix} + \epsilon\begin{bmatrix} 0 \\ -\dfrac{p_1}{\epsilon}y + \dfrac{q}{\epsilon}\cos\omega t\end{bmatrix}, \qquad (3)$$

and remarked that if a forcing term together with a dissipative term are added to $\dot{\mathbf{x}} = F_0(\mathbf{x})$, then the stable and unstable manifolds may have a homoclinic intersection, and hence an infinity of subsequent intersections, which causes the chaotic behavior of the oscillator to take place. In order to achieve parametrically excited oscillations, he let the parameter $p \to p(1 + \eta\cos\Omega_p t)$, where Ω_p is a modulation or variation frequency. Taking into account the perturbation, Eq. (3) becomes

$$\begin{bmatrix}\dot{x}\\ \dot{y}\end{bmatrix} = \begin{bmatrix} y \\ x - p(1 + \eta\cos\Omega_p t)x^3\end{bmatrix} + \epsilon\begin{bmatrix} 0 \\ -\dfrac{p_1}{\epsilon}y + \dfrac{q}{\epsilon}\cos\omega t\end{bmatrix}. \qquad (4)$$

In general, stronger perturbations are necessary to produce measurable control effects. For example, for a set of parameters (p, q, p_1), η has to be greater than some critical value, η_{critical}, in order for the homoclinic intersection between the stable and unstable manifolds to be suppressed. For the set of parameters $q = 0.088$, $p_1 = 0.154$, $\omega = 1.1$ and $p = 4$, he used $\eta = 0.03$. The interesting consequence of varying p to $p(1 + \eta\cos\Omega_p t)$ can be observed from the Ω_p–λ characteristics, where λ is the maximal Lyapunov exponent which indicates the presence and strength of the chaos of the system. When some "resonance" condition is satisfied,

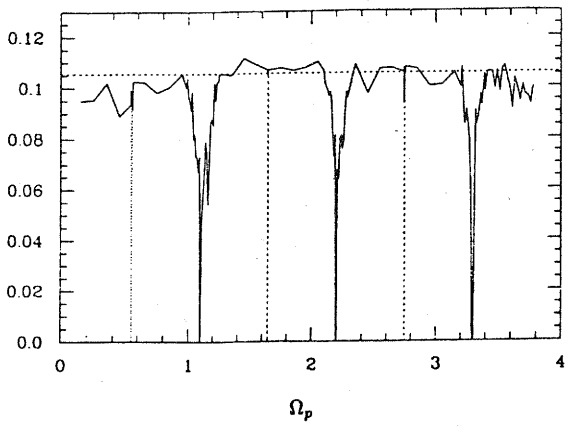

Fig. 1. Maximal Lyapunov exponent (λ) vs. parameter variation frequency (Ω_p). (*Figure from Pettini [1988], courtesy of Springer-Verlag.*)

a small relative variation of p is effective in reducing the chaos in the Duffing oscillator. As shown in Fig. 1, the suppression of chaos occurs ($\lambda = 0$) when the perturbation on p is introduced with a suitable frequency. For all the principal resonance cases, i.e., at the first, second, and third harmonics of Ω_p^0 and so on, set $\Omega_p = \Omega_p^0, 2\Omega_p^0, 3\Omega_p^0, \ldots$, where $\Omega_p^0 = \omega = 1.1$ for this particular set of parameters. As for the other cases of subharmonics of Ω_p^0, like $\Omega_p = \frac{1}{2}\Omega_p^0 = 0.55$ or $\Omega_p = 2\Omega_p^0 + \frac{1}{2}\Omega_p^0 = 2.75$, the chaos is substantially reduced, although not completely eliminated. Pettini concluded that a 3% modulation of a parameter is able to make the chaotic dynamics regular, when the modulation frequency Ω_p is resonant with the forcing frequency ω.

2.2. *Parameter perturbation methods*

In 1990, Ott, Grebogi & Yorke [1990] developed a more general method to control a nonlinear system by stabilizing one of the unstable periodic orbits embedded in its chaotic attractor, via small time-dependent perturbations of a variable system parameter.

Their idea comes from the observation that a chaotic attractor typically has embedded within it a dense set of unstable periodic orbits. A heuristic reasoning led them to the attempt of bringing any of these orbits to a periodic one by continuously applying small forces that would do the job. Their general control technique has prompted some more research work on this topic. In the following, we first describe the general approach of Ott *et al.*, and then its variants and modifications suggested by other researchers.

2.2.1. *The original approach*

To facilitate the presentation, denote the continuous-time autonomous system by

$$\dot{\mathbf{x}}(t) = F(\mathbf{x}(t), p)\,, \tag{5}$$

where p is a system parameter accessible for external adjustment within a small range, say $p^* - \Delta p_{\max} < p < p^* + \Delta p_{\max}$ with $\Delta p_{\max}$ being the maximal allowable perturbation. Suppose that when $p = p^*$ the system is chaotic.

Let ξ be the coordinates of the Poincaré map (surface of section), namely:

$$\xi_{n+1} = P(\xi_n, p)\,,$$

or

$$\xi_{n+1} = P(\xi_n, p_n)\,, \tag{6}$$

with $p_n = p^* + \Delta p_n$, $|\Delta p_n| \leq \Delta p_{\max}$ if p is assumed to be adjustable at every iteration of the mapping. For simplicity, assume that the continuous-time system described by Eq. (5) is three-dimensional, so that the corresponding surface of section is two-dimensional. One may then determine from the map many distinct unstable periodic orbits within the chaotic attractor and may select the periodic orbit that maximizes certain system performance which is defined according to the dynamic behavior of the system. For example, one may choose to pick a higher-order orbit as the desired one since it visits more regions of the attractor, and this can be advantageous because different regions correspond to different physical states of the system. In addition, one may like to pick as many of them as possible.

Assume that $\xi_F^* = P(\xi_F^*, p^*)$ is selected as the desired unstable fixed point of the map P, corresponding to the desired unstable periodic orbit of the system F. Then the iterations of the map near the desired orbit are observed and the local properties of this chosen periodic orbit are obtained. To do this, one needs to fit the iterations of the map (near the desired orbit) to a local linear approximation of the map. A first-order approximation of P near ξ_F^* and p^* is given by

$$\xi_{n+1} \simeq \xi_F^* + L(\xi_n - \xi_F^*) + \mathbf{w}(p_n - p^*)\,, \tag{7}$$

or

$$\Delta\xi_{n+1} \simeq L\Delta\xi_n + \mathbf{w}\Delta p_n\,, \tag{8}$$

where $\Delta\xi_n = \xi_n - \xi_F^*$, $\Delta p_n = p_n - p^*$, $L = (\partial/\partial\xi_n)P(\xi_F^*, p^*)$, and the partial derivative of the orbit (w.r.t. p) is $\mathbf{w} = (\partial/\partial p_n)P(\xi_F^*, p^*)$. The stable and unstable eigenvalues, λ_s and λ_u satisfying $|\lambda_s| < 1 < |\lambda_u|$, can be extracted from the approximate local linear map L. The stable and unstable manifolds, denoted M_s and M_u, are defined as those trajectories which converge asymptotically to the fixed point in a forward and backward time propagation process respectively, namely: M_s for $t \to +\infty$ and M_u for $t \to -\infty$. The directions of the local stable and unstable manifolds of the fixed point are given by the eigenvectors $\mathbf{e}_s$ and $\mathbf{e}_u$ corresponding to λ_s and λ_u respectively. If $\mathbf{f}_s$ and $\mathbf{f}_u$ are the contravariant basis vectors defined by $\mathbf{f}_s \cdot \mathbf{e}_s = \mathbf{f}_u \cdot \mathbf{e}_u = 1$ and $\mathbf{f}_s \cdot \mathbf{e}_u = \mathbf{f}_u \cdot \mathbf{e}_s = 0$, one can write $L = \lambda_u \mathbf{e}_u \mathbf{f}_u^\top + \lambda_s \mathbf{e}_s \mathbf{f}_s^\top$.

The dominant theme of the method of Ott *et al.* is to monitor the system until its trajectory comes *near* the desired orbit, i.e., till ξ_n falls close enough to ξ_F^*, and then to change the nominal value p^* of the parameter p by a small amount Δp, thereby changing the location of the orbit and its stable manifold such that the next iteration (represented by ξ_{n+1} in the surface of section) is forced back to the local stable direction (manifold) of the original fixed point ξ_F^*. For the case of a saddle-type fixed point, a figure given in Ditto, Rauseo & Spano [1990] is very illustrative and is redrawn here (Fig. 2) with only minor changes.

Now, assume that ξ_n has come sufficiently close to ξ_F so that Eq. (8) holds. For the next iteration ξ_{n+1} to fall onto the local stable manifold of ξ_F^*, the parameter $p_n = p^* + \Delta p_n$ has to be chosen such that the requirement $\mathbf{f}_u \cdot \Delta\xi_{n+1} = \mathbf{f}_u \cdot (\xi_{n+1} - \xi_F^*) = 0$ is satisfied. Taking the inner product of Eq. (8) with $\mathbf{f}_u$ gives

$$\Delta p_n = -\lambda_u \frac{\mathbf{f}_u \cdot \Delta\xi_n}{\mathbf{f}_u \cdot \mathbf{w}}, \tag{9}$$

where it is assumed that $\mathbf{f}_u \cdot \mathbf{w} \neq 0$. It should be noted that this calculated Δp_n is used to perturb the parameter p only if $\Delta p_n \leq \Delta p_{\max}$. When $\Delta p_n > \Delta p_{\max}$, however, the perturbation should be set to zero. Also, when ξ_{n+1} falls on the stable manifold of ξ_F^*, the perturbation Δp_n could be set to zero. The orbit for the subsequent time instants (i.e., ξ_{n+2}, $\xi_{n+3}, \ldots$) is then supposed to approach ξ_F^* with a geometrical rate λ_s. However, due to the errors or inaccuracies incurred in the above calculation and linearization, the subsequent iterations may tend to fall off the stable manifold instead. Therefore, a new Δp_n has to be calculated for every iteration to make sure that the subsequent ξ_n is approaching ξ_F^*. The above conjecture was tested on a popular dynamical model, the Hénon system, as shown in Ott, Grebogi & Yorke [1990].

In practice, exact mathematical formulation is often impossible because of the complex and uncertain nature of the processes and disturbances. For the previously described method of Ott *et al.*, the most important feature overall is that it does not require any model equation for the nonlinear system. As a matter of fact, all the values needed to calculate the control law can be obtained from experimental data by the so-called embedding technique. To be more specific, suppose that the global dynamical equations of the system, i.e., Eqs. (5), are unknown, but the experimental time series $z(t)$ can be measured. Then a delay-coordinate vector, called an embedding vector, can be formed as

$$\mathbf{Z}_\mathbf{x}(t) = [z(t),\, z(t-\tau), \ldots,\, z(t-(d-1)\tau)]^\top, \tag{10}$$

where τ is the time-delay and d the embedding dimension. The embedding vector provides enough information to characterize the essence of the system and can be used to obtain an experimental Poincaré map, hopefully a faithful one. For

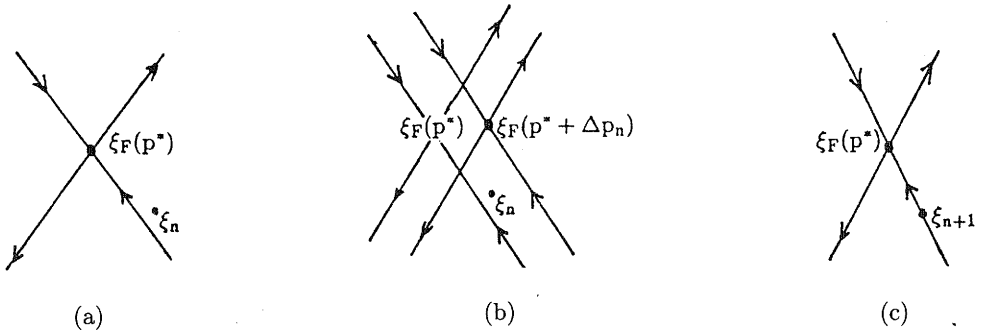

Fig. 2. The schematic of the parameter variation algorithm. (*This figure is redrawn based on a picture in Ditto, Rauseo & Spano [1990].*)

example, one may let the map be the equation of the first component of $\mathbf{Z}_{\mathbf{x}}(t)$ being equal to a constant: $z(t_n) =$ constant. This procedure yields the successive points $\xi_n := [z(t_n - \tau), \ldots, z(t_n - (d-1)\tau)]^\top$ of the map, where ξ_n denotes the coordinates in the map at the nth piercing of the map by the orbit [or, the vector $\mathbf{Z}_{\mathbf{x}}(t)$] and t_n is the time instant at the nth piercing. It is then a straightforward process to locate the periodic orbits from the experimental data. And the stable and unstable eigenvalues and manifolds of the surface of section, at the chosen fixed point of the map, may all be experimentally determined. Varying p slightly and observing how the desired fixed point changes its position, one can also estimate the partial derivative of the map with respect to p. In so doing, all the necessary values needed for calculating the perturbation value Δp_n have been obtained.

The advantage that no dynamical equations are needed seems to allow for the control of any chaotic system, provided that a faithful nonlinear map (Poincaré map) can be constructed for the system dynamics. This method has attracted the attention of many physicists studying nonlinear dynamics. Ditto, Rauseo & Spano [1990], for example, demonstrated the first successful process for the control of chaos in a real physical system, using the control mechanism introduced by Ott *et al.* They have been working with the so-called "smart materials," which often have nonlinear reactions to applied forces. Their experimental system consists of a gravitationally buckled, amorphous magnetoelastic ribbon placed within three mutually orthogonal pairs of Helmholtz coils. The ribbon changes its stiffness in the presence of the varying magnetic field of the coils, giving rise to nonlinear oscillations. They first created a map of the ribbon's chaotic attractor by tracking its changing posture. A periodic orbit was then picked from this attractor. When the ribbon came close enough to that particularly chosen orbit, they applied a small adjustment to the parameter H_{dc} of the vertical magnetic field, $H = H_{dc} + H_{ac}\cos(2\pi f t)$. They have been able to control the chaotic oscillations of the ribbon, observing stable period-1 and period-2 orbits in the chaotic regime. These are illustrated in Fig. 3.

Peng, Petrov & Showalter [1991] later studied an application of the same control method within the context of chemical chaos. The underlying nonlinear system is a three-dimensional chemical model, which has six reaction steps of rates given by law-of-mass-action kinetics. The results of their simulation

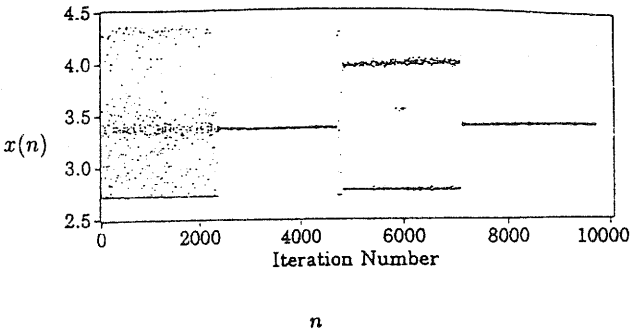

Fig. 3. Behavior of $x(n)$ as the system is switched from no control to control about the fixed point, then to control about periodic orbit, and finally back to control about the fixed point. (*Figure from Ditto, Rauseo & Spano [1990], courtesy of The American Physical Society.)*

may have some implication (of controlling chaos) to chemical or biological systems.

It is worth mentioning that Shinbrot, Ott, Grebogi, and Yorke have further studied how parameter variation procedure can speed up the travel of the system state from one position to another [say, from $\mathbf{x}_s$ to $\mathbf{x}_t$ for the system described by Eq. (5)], and a quantitative analysis is given to calculate the time needed for achieving the control [Shinbrot *et al.*, 1990]. Note that this procedure takes advantage of the extreme sensitivity of a chaotic system to small changes of the system parameter(s).

Consider the Poincaré map represented by Eq. (6). On this map, a point ξ_s is obtained by following the trajectory of Eq. (5) from $\mathbf{x}_s$ forward in time until the trajectory first intersects the surface of section, and let ξ_t be the first intersection point in the surface when the trajectory moves through $\mathbf{x}_t$ backward in time. Let $\overline{\varepsilon_t}$ denote a very small region (of linear size ε_t) around the target point ξ_t (Fig. 4).

Without any adjustment on the parameter p, the amount of time needed for traveling on the surface of section from ξ_s to the vicinity of ξ_t is $\tau \sim (1/\mu(\overline{\varepsilon_t}))$, where μ is the natural probability of the chaotic set, or

$$\tau \sim \left(\frac{1}{\varepsilon_t}\right)^D , \tag{11}$$

if the probability scales with Lyapunov information dimension D, indicating that τ increases according to a power law as the size ε_t decreases.

The procedure of Shinbrot *et al.* assumes that the parameter p is allowed to be varied; it involves forward-backward iterations. Let λ_+ and λ_- be the

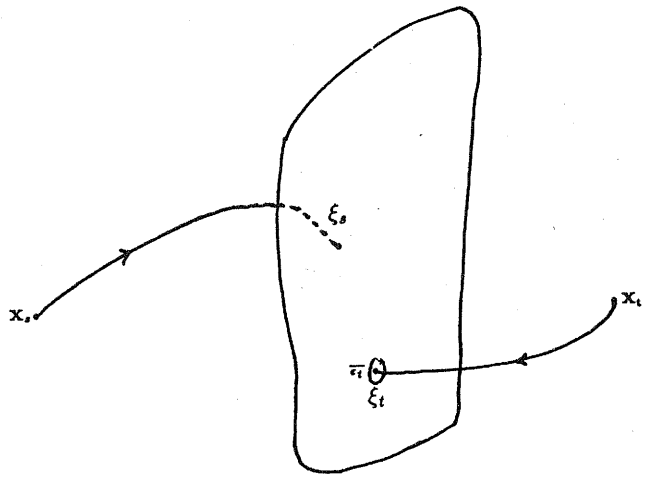

Fig. 4. Obtaining ξ_s and ξ_t on the Poincaré map.

positive and negative Lyapunov exponents obtained for typical initial conditions on the attractor for the map P, and assume that the size of the ergodic region of the mapping [Eq. (6)] is of order 1. After the first iteration of the map P, we have

$$\Delta\xi_1 \simeq \left.\frac{\partial P(\xi_s, p)}{\partial p}\right|_{p=p^*} \Delta p_1 \,, \tag{12}$$

which is the length of a small line segment, denoted $\overline{\Delta\xi_1}$, through the point $P(\xi_s, p^*)$. One may then iterate $\overline{\Delta\xi_n}$ forward (with $\Delta p_n = 0$) until $\Delta\xi_n$ stretches to a length of order 1 (i.e., the same order as that of the ergodic region), which occurs when $\Delta\xi_n e^{n_1\lambda_+} \sim 1$, where n_1 is the number of forward iterates used, and the time for the forward iteration is $\tau_1 \sim n_1 \sim (1/\lambda_+)\ln(1/\Delta\xi_n)$. Similarly, we iterate the region $\overline{\varepsilon_t}$ backward for n_2 times until this iteration first intersects the above forward iteration of $\overline{\Delta\xi_n}$, and the time is $\tau_2 \sim n_2 \sim (1/|\lambda_-|)\ln(1/\varepsilon_t)$. Finally, iterating a point in the middle of this intersection backward for n_1 times will lead to a point on $\overline{\Delta\xi_1}$, which is mapped to $\overline{\varepsilon_t}$ in $n_1 + n_2$ iterations. This allows us to find Δp_1 through Eq. (12).

Once Δp_1 is determined, and $\Delta p_n = 0$ for $n = 2, 3, 4, \ldots$, the time for mapping from ξ_s to $\overline{\varepsilon_t}$ is

$$\tau' = \tau_1 + \tau_2 \sim \frac{1}{\lambda_+}\ln\left(\frac{1}{\Delta\xi_n}\right) + \frac{1}{|\lambda_-|}\ln\left(\frac{1}{\varepsilon_t}\right), \tag{13}$$

as compared to the power law, Eq. (11). Note that for very small $\Delta\xi_n$ and ε_t, $n_1 \simeq \tau_1$ and $n_2 \simeq \tau_2$.

Note that this algorithm is also effective in the presence of small noise or small modeling error, as long as the variation Δp_n is applied at each iteration.

2.2.2. *An extension to the original approach*

In a more recent paper Nitsche & Dressler [1992] extended the general control approach of Ott *et al.* to accommodate the situation where the time-delay coordinates are used to reconstruct the attractor from a time series. For the application to experimental systems, they proposed some modified versions of the original control algorithm, where their argument is that, during the control process, the parameter p is varied from p_{n-1} to p_n at instant t_n, and if the time-delay coordinates are used to obtain the experimental surface of section, the map P, then this map will depend not only on the current parameter value p_n but also on the previous one, p_{n-1}, namely,

$$\xi_{n+1} = P(\xi_n, p_{n-1}, p_n)\,, \tag{14}$$

with the assumption that $t_{n+1} - t_n > (d-1)\tau$, i.e., the time distance between any two successive intersections of the surface of section is bigger than the time-lag window. In the case that only $2(t_n - t_{n-1}) > (d-1)\tau$ is satisfied, the experimental surface of section should take the form

$$\xi_{n+1} = P(\xi_n, p_{n-2}, p_{n-1}, p_n)\,. \tag{15}$$

Linearization of Eq. (14) results in

$$\Delta\xi_{n+1} \simeq L\Delta\xi_n + \mathbf{v}\Delta p_{n-1} + \mathbf{u}\Delta p_n\,, \tag{16}$$

where

$$L = \frac{\partial}{\partial\xi_n}P(\xi_F^*, p^*, p^*)\,, \quad \mathbf{v} = \frac{\partial}{\partial p_{n-1}}P(\xi_F^*, p^*, p^*)$$

and

$$\mathbf{u} = \frac{\partial}{\partial p_n}P(\xi_F^*, p^*, p^*)\,.$$

The requirement that $\mathbf{f}_u \cdot \Delta\xi_{n+1} = 0$ then leads to the following formula for perturbation:

$$\Delta p_n = -\lambda_u\frac{\mathbf{f}_u \cdot \Delta\xi_n}{\mathbf{f}_u \cdot \mathbf{u}} - \Delta p_{n-1}\frac{\mathbf{f}_u \cdot \mathbf{v}}{\mathbf{f}_u \cdot \mathbf{u}} \quad (\mathbf{f}_u \cdot \mathbf{u} \neq 0)\,, \tag{17}$$

which is a straightforward extension of the one given by Ott, Grebogi & Yorke [1990]. Note here that for simplicity, Eq. (6) is assumed to be two-dimensional as it was in Sec. 2.2.1. As a remedy for possible instability in the case that $|(\mathbf{f}_u \cdot \mathbf{v})/(\mathbf{f}_u \cdot \mathbf{u})| \geq 1$,

which causes the growing of Δp_n, Nitsche and Dressler suggested the requirements

$$\begin{cases} \mathbf{f}_u \cdot \Delta\xi_{n+2} = 0\,, \\ \Delta p_{n+1} = 0\,. \end{cases} \tag{18}$$

That is, at the time step t_n the control algorithm should stabilize the step only at t_{n+2} but not at t_{n+1}. Moreover, the next control parameter change should be zero. The perturbation formula then becomes

$$\begin{aligned} \Delta p_n = &-\lambda_u^2 \frac{\mathbf{f}_u \cdot \Delta\xi_n}{\lambda_u \mathbf{f}_u \cdot \mathbf{u} + \mathbf{f}_u \cdot \mathbf{v}} \\ &- \lambda_u \Delta p_{n-1} \frac{\mathbf{f}_u \cdot \mathbf{v}}{\lambda_u \mathbf{f}_u \cdot \mathbf{u} + \mathbf{f}_u \cdot \mathbf{v}} \\ &(\lambda_u \mathbf{f}_u \cdot \mathbf{u} + \mathbf{f}_u \cdot \mathbf{v} \neq 0)\,. \end{aligned} \tag{19}$$

Note that for the same reason which was stated in Sec. 2.2.1., this perturbation has to be calculated for every $n = 1, 2, \ldots$.

The modified algorithms, Eqs. (17) and (19), were tested on a simulation model of the Duffing equation $\ddot{x} + p_1\dot{x} + x + x^3 = q\,\cos\,\omega t$. When written as

$$\begin{cases} \dot{x}_1 = x_2\,, \\ \dot{x}_2 = -p_1 x_2 - x_1 - x_1^3 + q\,\cos\,\omega x_3\,, \\ \dot{x}_3 = 1\,, \end{cases}$$

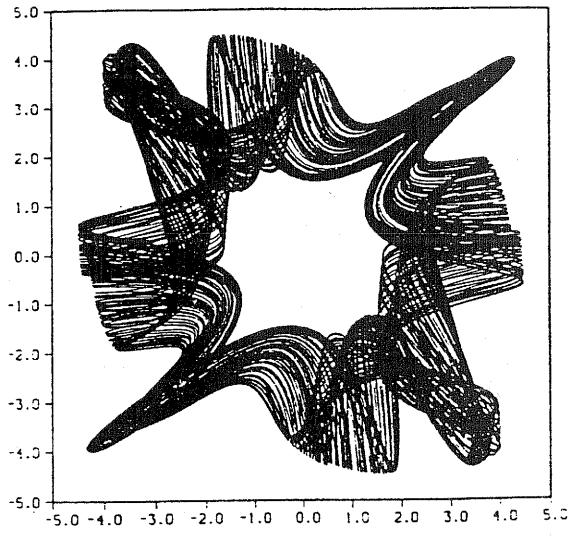

Fig. 5. A two-dimensional projection $[z(t-\tau),\, z(t)]^\top$ of the chaotic attractor in the three-dimensional embedding space. Poincaré map is picked at $z(t_n) = 1$. (*Figure from Nitsche & Dressler [1992], courtesy of Elsevier Science Publishers.*)

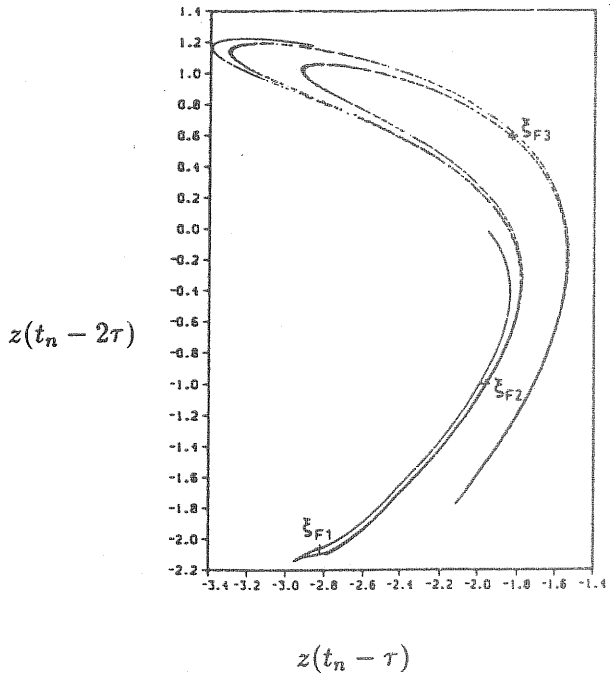

Fig. 6. The chaotic attractor in the two-dimensional Poincaré map $\xi_n = [z(t_n - \tau),\, z(t_n - 2\tau)]^\top$ and the three unstable fixed points $\xi_{F_1}, \xi_{F_2}, \xi_{F_3}$ embedded in the attractor. (*Figure from Nitsche & Dressler [1992], courtesy of Elsevier Science Publishers.*)

the equation was numerically integrated and its displacements $x_1 = x$ were taken as experimental time series, while the attractor was reconstructed using delay coordinates. In the simulation, the control parameter was chosen to be $p = q$. The original and modified control algorithms were then used to stabilize the fixed point determined from the reconstructed surface of section. When the influence of the preceding variation Δp_{n-1} is small, the effectiveness of the original algorithm [Eq. (9)] and the two modified ones [Eqs. (17) and (19)] turn out to be about the same. Otherwise, the modified versions work remarkably better (Figs. 5–8).

2.2.3. *A diode resonator*

Realizing a (large) N-periodic orbit in a chaotic system usually involves more than one correction in the long period. Multiple corrections are often necessary, unless the N-period cycle is itself stable or nearly stable.

In 1991, Hunt [1991] studied the parametric variation method on a physical system, a driven diode resonator. In this investigation, he has been able to convert the chaotic dynamics of the system into stable orbits with periods up to 23-driving

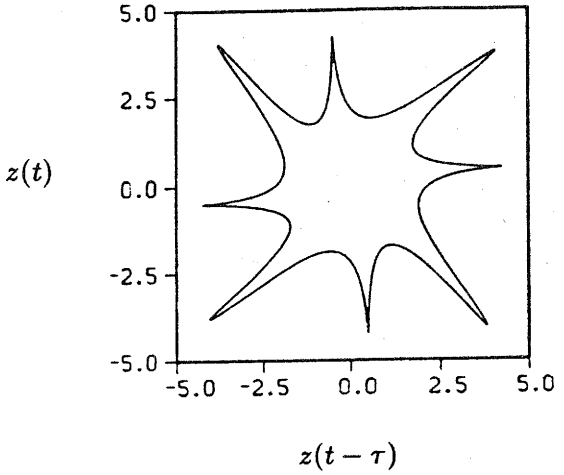

Fig. 7. A two-dimensional projection $[z(t-\tau), z(t)]^\top$ of the periodic orbit plotted in the three-dimensional embedding space (The periodic orbit corresponds to the ξ_{F_2} in Fig. 6.) (*Figure from Nitsche & Dressler [1992], courtesy of Elsevier Science Publishers.*)

cycles. The system under investigation has a p-n junction rectifier diode cascaded with an inductor. When driven by an appropriate sinusoidal voltage, the system exhibits chaotic phenomena. The block diagram of this system is reproduced in Fig. 9.

Within a specified window, the difference between the chaotic variable and a set point is used to perturb the controlling drive. The system trajectory may tend to stable orbits by itself. To find these different orbits, one only needs to vary the window, the set point, and the amplitude of the amplifier. What makes his approach different from that of Ott, Grebogi & Yorke [1990] is that relatively large perturbations are allowed in this method, so that high-period orbits can be handled. Essentially a one-dimensional version of the algorithm by Ott *et al.*, this approach has some conventional control engineering flavor since it employs occasional proportional feedback (OPF).

As shown in Fig. 10, the peak current through the diode is sampled as I_n. If I_n is out of the range of the window, no modulation signal is applied. When I_n falls within the preset window, however, the drive voltage is amplitude-modulated with a signal proportional to the difference between I_n and the center of the window, thereby achieving the control of the chaotic signal. The difference between I_n and the center of the window is passed through an amplifier and so becomes the drive voltage signal which then amplitude-modulates the signal generator, achieving the control purpose. Yet for low-period orbits, their approach seems to be more experimental than systematic. It is not guaranteed that some particular periodic orbits (e.g., those with period-13, 14, 15 and 17, as mentioned in Hunt [1991]) can be stabilized. It is worth mentioning that recently the OPF method or similar approaches were employed to control chaos in a globally-coupled, multimode, autonomous laser system and in fiber lasers [Roy *et al.*, 1992; Glorieux *et al.*, 1992].

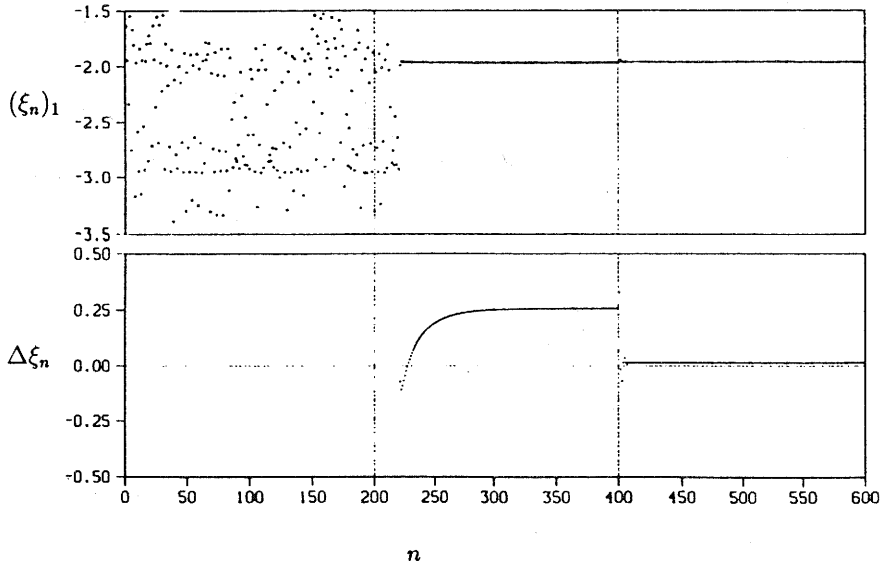

Fig. 8. The process of stabilizing ξ_{F_2} is shown by the behavior of the first component $(\xi_n)_1$ of the points in the map. Three control laws are initiated successively: Eq. (9) for $n = 0, \ldots, 200$; Eq. (17) for $n = 201, \ldots, 400$; Eq. (19) for $n = 401, \ldots, 600$. (*Figure from Nitsche & Dressler [1992], courtesy of Elsevier Science Publishers.*)

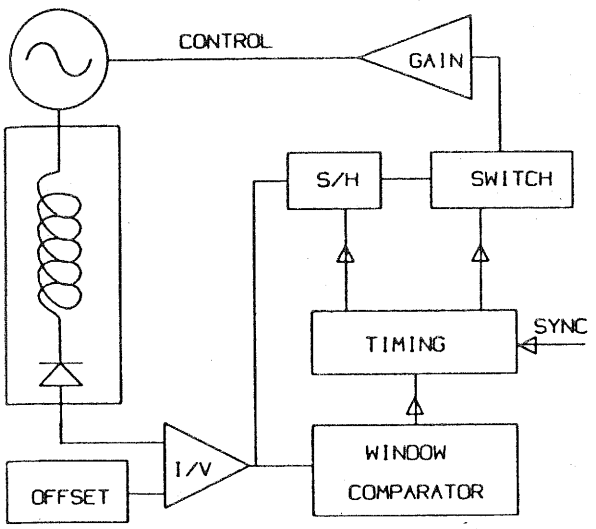

Fig. 9. Block diagram of the diode resonator system. (*Figure from Hunt [1991], courtesy of the American Physical Society.*)

(a)

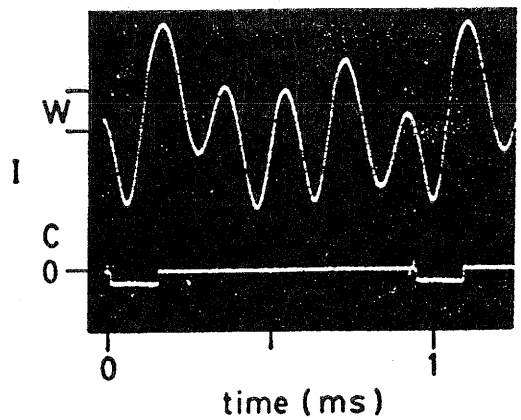

(b)

Fig. 10. (a) Double exposure showing the first return map (I_{n+1} vs. I_n), in which the five overexposured dots represent the period-5 orbit. (b) Upper trace – current through resonator. Lower trace – control signal C. (*Figure from Hunt [1991], courtesy of The American Physical Society.*)

3. Entrainment and Migration Controls

Another representative approach for the control of chaos is referred to as the so-called entrainment and migration control methods, proposed by Jackson [1990, 1991a], Hübler [1987, 1989], and their colleagues, Hübler & Lüscher [1989], Plapp & Hübler [1990], Jackson & Hübler [1990], and Jackson & Kodogeorgiou [1991]. This general approach has been successfully applied to many complex dynamic systems such as multi-attractor systems [Jackson, 1991a], multi-periodic forcing control of the one-dimensional logistic map [Jackson, 1990], a Gaussian-related map [Jackson, 1991a], and the two-dimensional Hénon and Ikeda maps [Jackson & Kodogeorgiou, 1991].

Complex dynamic systems are frequently associated with multi-attractors, possibly of different topological types, and many other complicated dynamical responses to the environment, which can be found in fluid and heat processes [Coles, 1965; Fenstermacher *et al.*, 1979; Glass *et al.*, 1986] optics [Lugiato, 1984], adaptive control processes [Mareels & Bitmead 1986, 1988; Hübler & Lüscher 1990; Sinha *et al.*, 1990], neural networks [Grassberger & Procaccia, 1984], and biological systems [Nicolis, 1987]. The entrainment and migration control strategy allows one to impose a variety of dynamic motions onto such complex systems. Unlike the parametric variation methods discussed in the previous section, this approach requires that the dynamics of the system can be accurately described either by a map or by an ordinary differential equation.

3.1. *Entrainment-goal control*

The entrainment control method was first introduced by Hübler [1987] and used by Hübler and Lüscher in the investigation of logistic maps and nonlinear damped oscillations [Hübler & Lüscher, 1989]. Based on Hübler's method and the results of Jackson & Hübler [1990], Jackson [1991a] described a generalized formulation of the approach and addressed the following issues: (1) To what kind of systems can this control method be applied? (2) Given a nonlinear dynamical system of a certain type, what kind of controls can be used? (3) What are the limitations in initializing such a control? (4) How to use this control method to transfer the trajectory of a multi-attractor system from one attractor to another?

The generalized formulation described by Jackson [1991a] was based on the existence of certain convergent regions in the phase space of a multi-attractor system. In each of these convergent regions, all the nearby orbits converge locally toward each other. An important observation is that although many of these attractors have positive Lyapunov exponents, they nevertheless have such regions in their basins of attraction where nearby orbits generally converge, meaning that the Lyapunov exponents are merely an average measure of their dynamics. Based on this observation and many well-studied examples, Jackson conjectured that every multi-attractor system has at least one convergent region within each basin of attraction. Moreover, in Jackson [1991b], he described a method for determining such convergent regions analytically by using the Routh–Hurwitz theorem, yet without explicitly finding the roots of the corresponding characteristic determinant, where the technique was successfully applied to both the Lorenz and the Rössler systems.

Presumably, these convergent regions exist. It is then possible to employ the system's intrinsic (local) dynamics to lead the orbits, say $\{x(n)\}$ in the discrete case, to approach (a limited set of) the desired dynamics $\{g(n)\}$ in the sense that

$$\lim_{n\to\infty} |x(n) - g(n)| = 0\,. \tag{20}$$

In so doing, the system is said to be "entrained" to this goal dynamics $\{g(n)\}$. The continuous version of entrainment is defined in a similar manner. The significance is that this goal dynamics can have any topological characteristic such as equilibrium, periodic, knotted, chaotic, etc., provided that the target orbit $\{g(n)\}$ is located in some goal region $\{G_n\}$ satisfying $G_n \cap C_n \neq \phi$, where C_n $(n = 1, 2, \ldots)$ are the aforementioned convergent regions which are system-dicated (a property of autonomous systems). For simplicity, assume that $G_n \subset C_n$ with the goal orbit $g(n) \in G_n \subset C_n$ $(n = 1, 2, \ldots)$. Let $C = \cup_{n=1}^{\infty} C_n$ and denote the basin of entrainment for the goal by

$$B = \left\{x(0) : \lim_{n\to\infty} |x(n) - g(n)| = 0\right\}. \tag{21}$$

The entrainment is reliable even if the initial state of the system (when the control is initialized) is only known to lie in a prescribed "macroscopic" basin B, and no information other than the initial states is needed. Once a near-entrainment is obtained in the sense that $|x(n) - g(n)| \leq \varepsilon$ for some small $\varepsilon > 0$, another form of control can be applied to use the migration-goal dynamics between different convergent regions. This allows the system trajectory to be transferred from one attractor to another. Moreover, the method is stable against certain degree of dynamical modeling error and noise disturbance.

To describe the method more precisely, consider a two-dimensional map of the form

$$\mathbf{x}_{n+1} = F(\mathbf{x}_n)\,, \quad \mathbf{x}_n \in R^2\,. \tag{22}$$

Let the goal dynamics be $\{\mathbf{g}_n\}$ and S_n be a switch indicator defined by $S_n = 0$, $n < 0$ and $0 \leq S_n \leq 1$ for $n \geq 0$. The controlled dynamic system was then proposed to be the following:

$$\mathbf{x}_{n+1} = F(\mathbf{x}_n) + S_n[\mathbf{g}_{n+1} - F(\mathbf{g}_n)]\,, \tag{23}$$

in which the control is initiated, with $S_n = 1$, if the system state has entered the basin B, i.e., $\mathbf{x}_n = \mathbf{x}_{n_c} \in B$. Observe that the control $\mathbf{u}_n := S_n[\mathbf{g}_{n+1} - F(\mathbf{g}_n)]$ is of open-loop type, which is directly added to the original system. Hence, it is neither any of the aforementioned parametric variation methods nor the closed-loop feedback control method to be introduced in the next section. Moreover, since $S_n = 1$, the above controlled system has actually reduced to

$$\mathbf{g}_{n+1} - F(\mathbf{g}_n) = \mathbf{x}_{n+1} - F(\mathbf{x}_n) = 0\,, \quad n = n_c, n_c+1, \ldots,$$

which implies that the desired goal orbit $\{\mathbf{g}_n\}$ has to satisfy the given system for $n \geq n_c$.

An important particular example of entrainment control is the one with the goal $\mathbf{g}_n \equiv \mathbf{g}_0$, an equilibrium point of the system. In this case, the basin of entrainment, B, is a convex region in the phase space and is given by

$$B = \{\mathbf{x}_0 : |\mathbf{x}_0 - \mathbf{g}_0| < r(\mathbf{g}_0)\}\,,$$

where

$$r(\mathbf{g}_0) = \max_r \left\{r : |\mathbf{x}_0 - \mathbf{g}_0| < r \to \lim_{k\to\infty} |\mathbf{x}_n - \mathbf{g}_0| = 0\right\}.$$

In order for the system trajectory to be entrained to the given equilibrium point $\mathbf{g}_0$, however, the equilibrium point must lie in a particular subset $\bar{C}$ of the convergent region C. For one-dimensional systems, a general necessary and sufficient condition for such "entrainability" (not restricted to equilibrium points) was provided by Jackson [1991a]: Let

a and b be two real numbers such that $a < x(0)$, $x_0 < b$, define

$$\bar{C} = \left\{ x_n : a < x_n < b, \max_{a<x_n<b} \left| \frac{\partial F}{\partial x} \right| < 1, M < \frac{(b-a)}{2} n \geq 0 \right\},$$

where

$$M = \max_{a<x_n,x_\ell<b} [F(x_n) - F(x_\ell)],$$

and denote

$$\bar{G} = \{g_n : g_n \in R, a + M < g_n < b - M, n \geq 0\}.$$

If $x_0 \in \bar{C}$ and

$$x_{n+1} = F(x_n) + g_{n+1} - F(g_n), \quad n = 0, 1, \ldots,$$

then $|x_n - g_n| \to 0$ as $n \to \infty$. Here, it is usually difficult to determine the subsets $\bar{C}$ and $\bar{G}$ since the conditions offered are "often over-conservative" [Jackson, 1991a].

For the so-called uniform entrainment, which is defined globally in the mean-value sense, Jackson [1991a] also provided an estimate for the maximum basin for the equilibrium point g_0: Assume that $F(\cdot)$ is piecewise differentiable and g_0 is in the convergent region C. Suppose also that there exist two real numbers $-\infty \leq a < b \leq \infty$ such that

$$|F(x_0) - F(g_0)| < |x_0 - g_0| \text{ for all } a < x_0 < b,\ x_0 \neq g_0,$$

and such that for finite values of a and b,

$$b - g_0 = |F(b) - F(g_0)| \text{ and } g_0 - a = |F(a) - F(g_0)|.$$

Then, denoting by $\{a^*, b^*\}$ the set of the roots of

$$\begin{cases} F(a^*) - F(g_0) = b - g_0, & a^* < g_0, \\ F(b^*) - F(g_0) = a - g_0, & g_0 < b^*, \end{cases}$$

the maximum basin of the uniform entrainment to g_0 is estimated by

$$B_{\max} = \{x_0 : \max(a, \{a^*\}) < x_0 < \min(b, \{b^*\})\}.$$

Jackson & Hübler [1990] studied the one-dimensional logistic map

$$x_{n+1} = cx_n(1 - x_n)$$

and found the basin of entrainment to its equilibrium point g_0 to be

$$B = \{x_0 : 1 - g_0 - c^{-1} < x_0 < g_0 + c^{-1}\}.$$

Outside the basin B, the solutions of the system tend to the attractor $x_{-\infty}$. This basin is shown in Fig. 11.

Jackson & Hübler [1990] also investigated the basin for a more complicated case where the goal dynamics is of period-two, $\{g_n\} = \{g_0, g_1, g_0, g_1, \ldots\}$. The basin in this case turns out to contain a few disjoint portions, as shown in Fig. 12. As

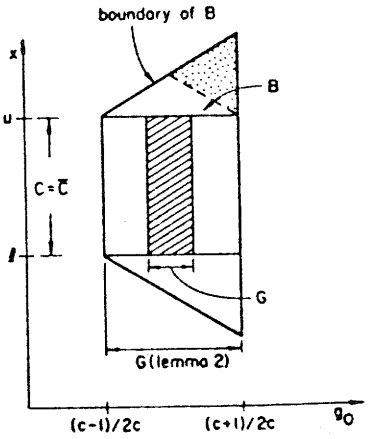

Fig. 11. Basin of entrainment of the one-dimensional logistic map. (*Figure from Jackson [1991a], courtesy of Elsevier Science Publishers.*)

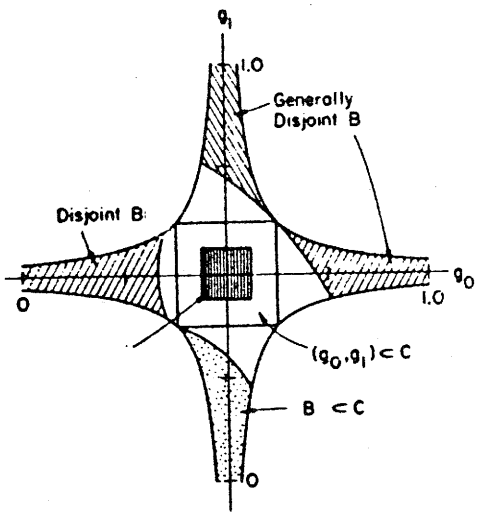

Fig. 12. Basin of entrainment of the logistic map with a period-2 goal. (*Figure from Jackson & Hübler [1990], courtesy of Elsevier Science Publishers.*)

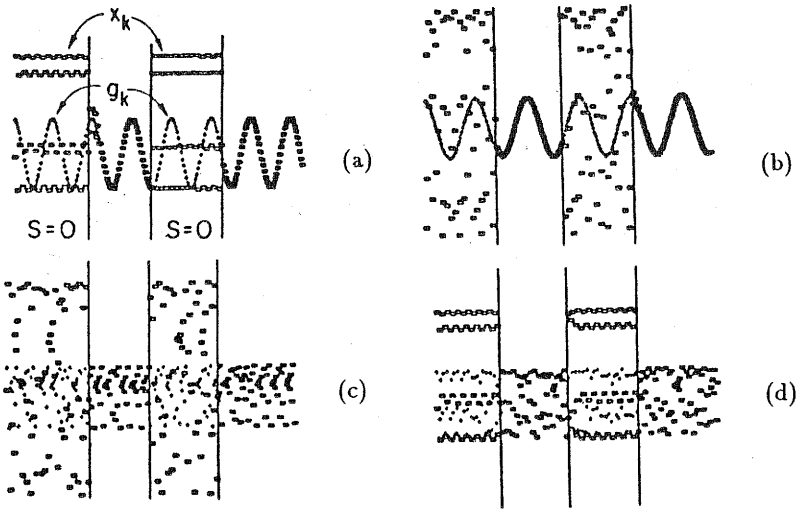

Fig. 13. Entrainment of the logistic map. (*Figure from Jackson [1991a], courtesy of Elsevier Science Publishers.*)

can be seen from the figure, the disjoint portions of the basin of entrainment constitute three arms from the convergent region, and the other basins which intersperse this basin of entrainment may be some bounded or unbounded periodic orbits. It is interesting to see that in the fourth arm of the figure, corresponding to $g_0 \approx 0.5$ and $g_1 \to 1$, the basin of entrainment is not disjoint from the stable region. Instead, it becomes vanishingly small.

The logistic map was used to illustrate the topological generality of the system's complex dynamics [Jackson, 1991a], as shown in Fig. 13, where all the goal dynamics $\{g_n\}$ are in the convergent region. The controls were initiated (with $S_0 = 1$) at the first and the third vertical lines and terminated (with $S_n = 0$) at the second line. The four figures (a)–(c) illustrate the system's transitions: (a) order → order, (b) chaos → order, (c) chaos → chaos, and (d) order → chaos.

3.2. *Migration-goal control*

The purpose of the so-called migration-goal control is to transfer the system dynamics from one convergent region, say C_i, to another, C_j $(i \neq j)$. There are many reasons for such a state transfer. For example, among the many attractors of a complex system, some may have very different types of dynamics (periodic, intermitric, chaotic, etc.) and one of them may be most beneficial to a particular behavior of the system. Thus, chaos may lead the system to self-destruction, so that periodic dynamics may be relatively "healthy." Conversely, regular (non-chaotic) dynamics may be "unhealthy" in the sense that they do not show sensitive response to a changing environment and hence do not provide enough information about the system behavior under certain circumstances.

In the migration-goal control, the strategy is again

$$\mathbf{x}_{n+1} = F(\mathbf{x}_n) + [\mathbf{g}_{n+1} - F(\mathbf{g}_n)]\,, \qquad n = 0, 1, \ldots, N-1\,, \quad (24)$$

where N is the switching time-index. Jackson [1991a] studied a Gaussian-related map described by

$$x_{n+1} = G(x_n; r) = \frac{1}{2} r e^{1/2} x_n e^{-2x_n^2}\,, \quad 2 \leq r \leq 8\,, \quad (25)$$

which is similar to the logistic map in the region $0 \leq x_n \leq 1/2$. This system has two attractors, A_1 (chaotic) and A_2 (periodic), and two bounded convergent region, C_1 and C_2, in the basin of attraction (which consists of two subregions B_1 and B_2), and two infinite convergent regions $C_\infty(1)$ and $C_\infty(2)$, as shown in Fig. 14. For example, if the system trajectory is in B_1 (attracted to A_1), one can choose the equilibrium point $g_0 \in C_2$ as the goal and then turn on the control, so that the trajectory $x_n \to g_0$.

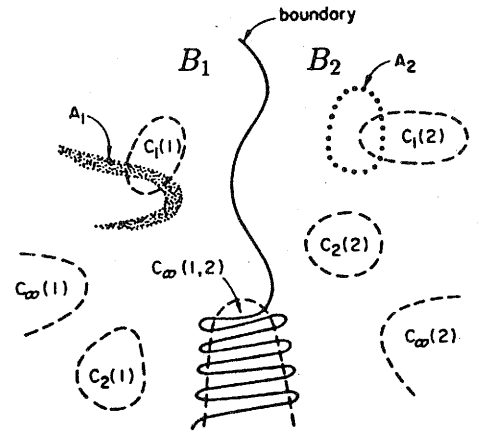

Fig. 14. Migration of the Gaussian-related map. (*Figure from Jackson [1991a], courtesy of Elsevier Science Publishers.*)

3.3. *Entrainment and migration of the Ikeda map*

In addition to the one-dimensional maps discussed above, Jackson & Kodogeorgiou [1992] have also studied the entrainment and migration control for an interesting two-dimensional map: the Ikeda map described by

$$\begin{cases} x_{n+1} = b(x_n \cos\theta_n - y_n \sin\theta_n), \\ y_{n+1} = b(x_n \sin\theta_n - y_n \cos\theta_n), \end{cases} \tag{26}$$

where $\theta_n = c - (d/1 + x_n^2 + y_n^2)$ with some constant parameters b, c and d. The corresponding controlled Ikeda system is

$$\begin{cases} x_{n+1} = b(x_n \cos\theta_n - y_n \sin\theta_n) + g_{n+1} - b(g_{x,n} \cos\phi_n - g_{y,n} \sin\phi_n), \\ y_{n+1} = b(x_n \sin\theta_n - y_n \cos\theta_n) + g_{n+1} - b(g_{x,n} \sin\phi_n - g_{y,n} \cos\phi_n), \end{cases} \tag{27}$$

where $\phi_n = c - (d/1 + g_{x,n}^2 + g_{y,n}^2)$. If the goal is taken to be the origin, $\mathbf{g}_0 = (g_{x,0}, g_{y,0}) = (0,0)$, and if $|b| < 1$, then it can be easily verified that the basin is the entire phase space R^2. Hence, the control can be initialized at any time. But if not, say when $\mathbf{g}_0 = (1,0)$, the basin of entrainment is very small and highly irregular, as shown in Fig. 15. A migration-goal control of the Ikeda system from a (strange) attractor A_1 to its equilibrium attractor A is illustrated in Fig. 16.

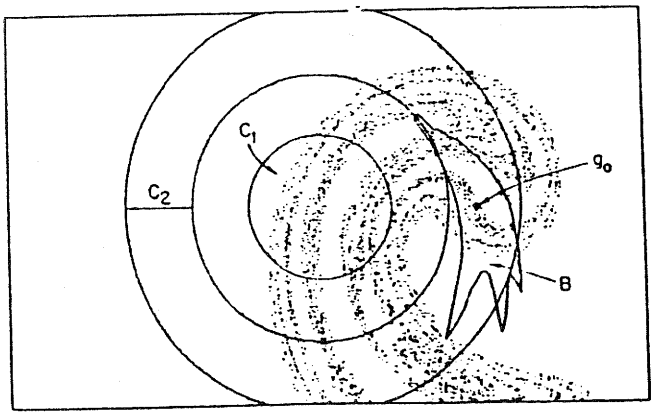

Fig. 15. Basin of entrainment of the Ikeda map. (*Figure from Jackson & Kodogeorgiou [1991].*)

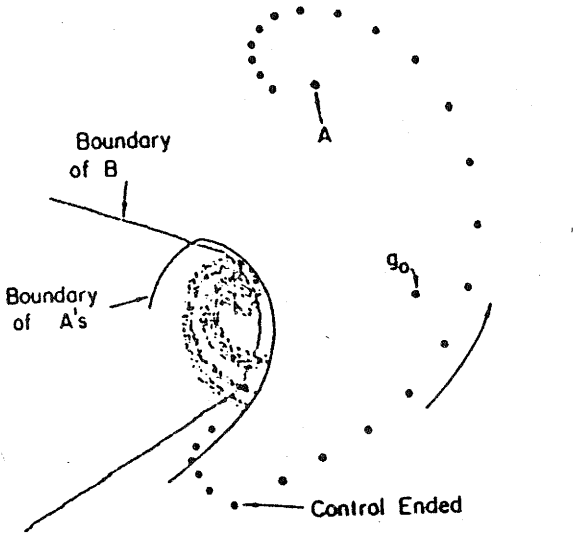

Fig. 16. Migration of the Ikeda map. (*Figure from Jackson & Kodogeorgiou [1992].*)

4. Engineering Control Approaches

Most of the control methods discussed in the previous sections were originally proposed by experimental and/or theoretical physicists and mathematicians, and none of them intentionally employs the conventional engineering control strategies. One may wonder whether there might be a more efficient

solution to controlling chaos, which makes use some of the well-developed control engineering methodologies. The answer is a qualified *Yes*, and there actually has been a number of publications in the literature which reported some success in this direction of research [Fowler, 1989; Vincent & Yu, 1991; Chen & Dong, 1992, 1993a; Dong & Chen, 1992a, 1992b]. This approach is important in that it not only offers a control engineering perspective to the control of chaos but may have also laid some ground work for a more systematic and comprehensive study of the subject. This section is to discuss such a control engineering approach, which, as will be seen, is in principle quite different from the aforementioned methods.

4.1. *To feedback or not*

Generally speaking, feedback controls, linear or not, have been recognized to be very useful for stabilizing an unstable system while tracking a reference input and/or rejecting uncertain disturbances, etc., see for example, Chui & Chen [1989, 1992] and deFigueiredo & Chen [1993].

Conventional feedback controllers are designed for nonchaotic systems. In particular linear feedback controllers are often designed for linear systems. That a self-adapting feedback system is resistant to chaotic signals is perhaps a statement that requires no justification to a dynamics analyst, but deriving a control algorithm that ensures the chaotic system trajectory stay at its unstable equilibria may not be trivial at all. A chaotic system's sensitivity to initial conditions may lead to the impression that in chaotic systems their sensitivity to small errors makes them very difficult, and probably impossible, to control using conventional feedback methods over all of their phase space. Such an impression may lead to the argument that once the control is initiated there is no need to further monitor the system's dynamics, nor to feedback this information in order to sustain the control. Indeed, it turns out that conventional feedback controls of chaotic systems are generally difficult, but not impossible, as will be seen shortly.

The motivations for using conventional feedback systems to control chaos include that feedback controllers are easy to implement, can perform the jobs automatically after being designed and implemented, can stabilize the overall control system efficiently, and usually have significant physical meanings.

The present authors have recently developed some new ideas and formalized some successful techniques for controlling (or ordering) chaotic discrete-time and continuous-time systems using conventional engineering feedback controls, based essentially on the rigorous Lyapunov arguments [Chen & Dong, 1992, 1993a; Dong & Chen, 1992a; 1992b, 1993b; Chen, 1993]. What have been achieved include: (1) controlling chaotic trajectories of some typical systems such as the discrete-time Lozi and Hénon systems and the continuous-time Duffing system and Chua's circuit; (2) controlling chaotic trajectories of such systems to their unstable equilibria and/or unstable limit cycles (even multi-periodic orbits); and (3) the feedback controller can be either nonlinear or linear. This section is devoted to a description of these basic ideas, design methods, and mathematical principles employed in the research, along with discussion on other engineering control approaches taken by other researchers.

4.2. *Controlling discrete-time and continuous-time chaotic systems via feedback*

The feedback control techniques are discussed in this section. Two representative examples, namely the Hénon and Lozi systems, are first studied, which are among the simplest second-order discrete-time nonlinear models. The control of a continuous-time system, the Duffing oscillator, is then discussed.

4.2.1. *Controlling the Lozi system*

The Lozi system is described by the following difference equations

$$\begin{cases} x_1(n+1) = f_1[x_1(n), x_2(n)] \\ \qquad\qquad = -p|x_1(n)| + x_2(n) + 1\,, \\ x_2(n+1) = f_2[x_1(n), x_2(n)] = qx_1(n)\,, \end{cases} \tag{28}$$

where p and q are two real parameters.

As simple as it is, Lozi system is rife with chaotic phenomena. Its two equilibrium points, when the system parameters p and q are restricted to be varied within certain range, are

$$\begin{cases} \bar{x}_1 = \pm\dfrac{1}{p \mp (q-1)}\,, \\ \bar{x}_2 = \pm\dfrac{q}{p \mp (q-1)}\,, \end{cases} \quad (p \mp (q-1) \neq 0)\,.$$

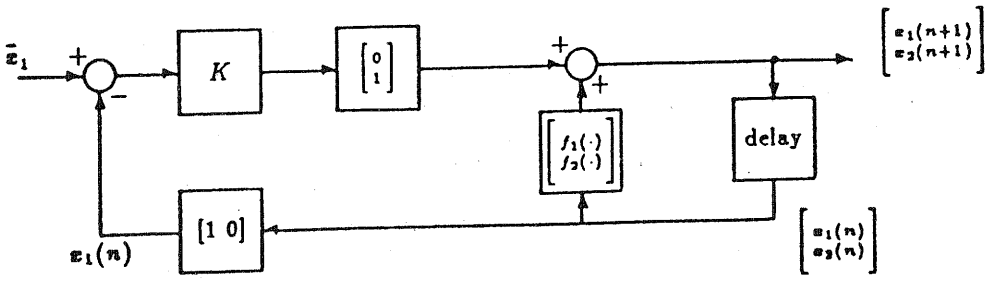

Fig. 17. Block diagram of the controlled Lozi system [f_1 and f_2 are defined in Eq. (28)]. (*Figure from Chen & Dong [1992].*)

Consider, as usual, the first (unstable) equilibrium point

$$(\bar{x}_1, \bar{x}_2) = \left(\frac{1}{p-(q-1)}, \frac{q}{p-(q-1)}\right), \qquad (29)$$

and observe that the determinant of the Jacobian $J|_{\bar{x}_1,\bar{x}_2}$ at this equilibrium point $(\bar{x}_1, \bar{x}_2)$ of the system is given by $\det[J|_{\bar{x}_1,\bar{x}_2}] = -q$, which shows that the behavior of the Lozi system depends sensitively on the parameter q. By varying the value of q, various patterns of a "strange attractor" can be observed [Chen & Dong, 1992]. For all such values of p and q, the system equilibrium point [Eq. (29)] is not a stable one since all the trajectories of the system are wandering near but never approach this equilibrium point.

Now consider the problem of designing a feedback controller to control the chaotic Lozi system and drive its trajectory to the equilibrium point $(\bar{x}_1, \bar{x}_2)$ shown above. To do so, as usually do in feedback systems design, one may input a control in the "canonical form" $\begin{bmatrix}0\\1\end{bmatrix}u(n)$ with a linear feedback controller $u(n) = -Kv(n)$ for some constant feedback gain K and some executive input $v(n)$. The following result has been established in Chen & Dong [1992]:

Proposition 1. *A necessary condition for the local controllability of the chaotic Lozi system to its equilibrium point* $(\bar{x}_1, \bar{x}_2)$ *given by* Eq. (29) *is*

$$v(n) \to 0 \quad as \quad n \to \infty,$$

where $u(n) = -Kv(n)$ *is the feedback controller applied to the system.*

Note that if the control is applied when the trajectory is within the basin, this condition is also sufficient [Chen & Dong, 1992].

Conceivably, one may choose the (perhaps simplest) control law

$$v(n) = x_1(n) - \bar{x}_1 .$$

Adding this control input to the original system yields the following "controlled Lozi system,"

$$\begin{cases} x_1(n+1) = -p|x_1(n)| + x_2(n) + 1, \\ x_2(n+1) = qx_1(n) - K[x_1(n) - \bar{x}_1]. \end{cases}$$

This feedback configuration is shown in Fig. 17.

Clearly, it is necessary to ensure that the controlled Lozi system be itself stable (otherwise, control cannot be performed and unexpected chaos may occur) and to achieve the goal of driving the chaotic trajectory of the system to the target. To determine the feedback control gain K the following sufficient condition has been obtained [Chen & Dong, 1992]:

Proposition 2. *A sufficient condition for a stable feedback control of the chaotic Lozi system in the form* $u(n) = -K[x_1(n) - \bar{x}_1]$, *where* $(\bar{x}_1, \bar{x}_2)$ *is the same targeting equilibrium point, is that*

$$\begin{cases} \max\{q - 1 - p \cdot \mathrm{sgn}(\bar{x}_1),\ q - 1 + p \cdot \mathrm{sgn}(\bar{x}_1)\} \\ \qquad < K < \dfrac{1}{4}(p^2[\mathrm{sgn}(\bar{x}_1)]^2 + 4q), \\ -2 < p < 2. \end{cases}$$

With this condition, the following computer simulations have been carried out in Chen & Dong [1992]: In Figs. 18(a)–18(d), $p = 1.8$ is fixed and $q = -1.0$, 0.4, 0.997, and 1.0 respectively. To control the chaotic trajectories to the targeting equilibrium point, we have, by Proposition 2, the following

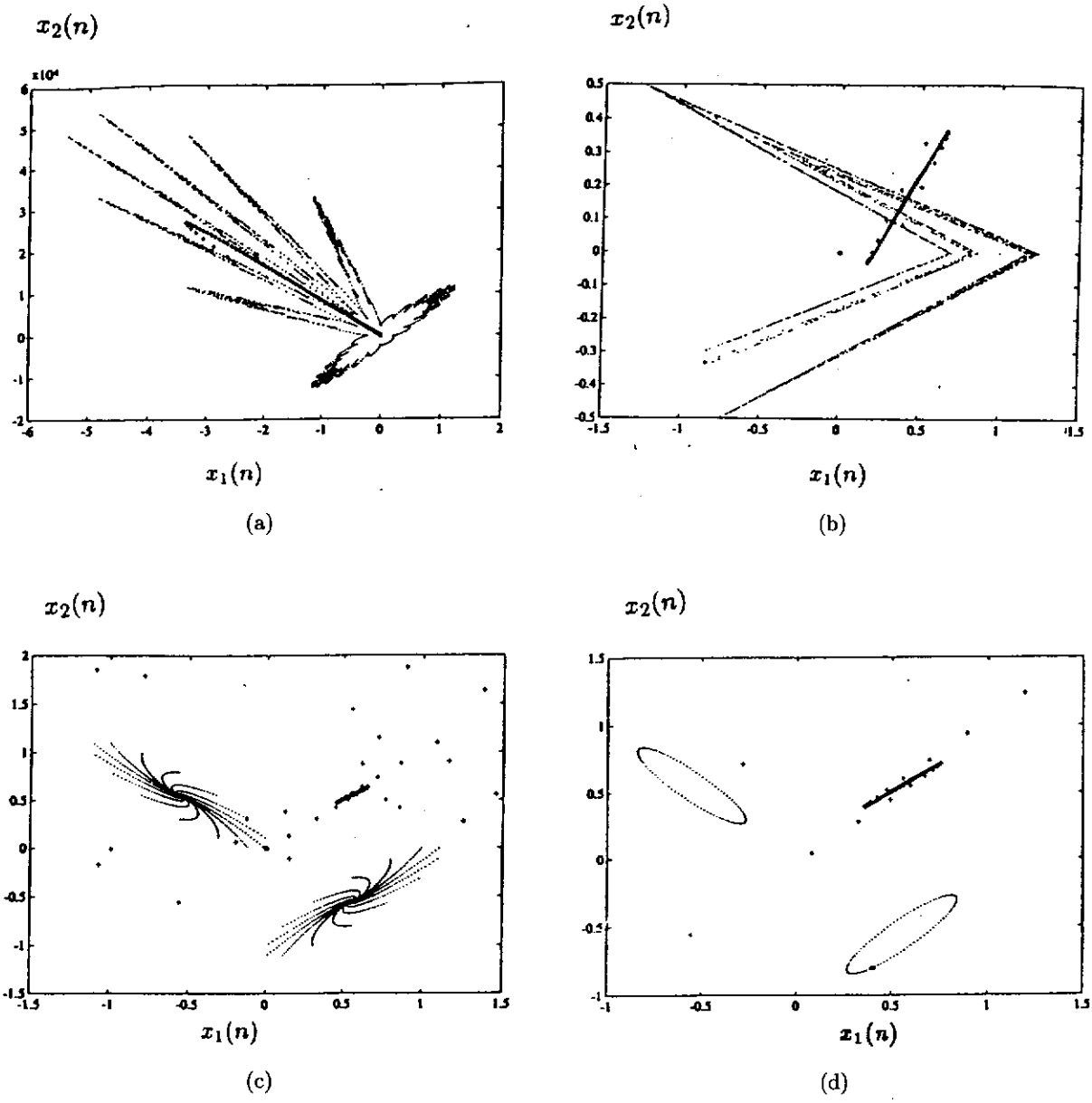

Fig. 18. Lozi system trajectory before and after feedback control is applied. (a) A Lozi system with ($p = 1.8$, $q = -1$), initial position (-5000, 5000), $N = 3000$, $Nc = 500$, $K = -0.195$. (b) A Lozi system with ($p = 1.8$, $q = 0.4$), initial position (0, 0), $N = 2500$, $Nc = 500$, $K = 1.205$. (c) A Lozi system with ($p = 1.8$, $q = 0.997$), initial position (0, 0), $N = 2500$, $Nc = 500$, $K = 1.802$. (d) A Lozi system with ($p = 1.8$, $q = 1$), initial position (0.4, -0.8), $N = 400$, $Nc = 200$, $K = 1.805$. (*Figure from Chen & Dong [1992].*)

bounds for the gain K:

$$\begin{aligned} -0.2 < K < -0.19 \quad & (K = -0.195 \text{ is used in Fig. 18(a)}), \\ 1.2 < K < 1.21 \quad & (K = 1.205 \text{ is used in Fig. 18(b)}), \\ 1.797 < K < 1.807 \quad & (K = 1.802 \text{ is used in Fig. 18(c)}), \\ 1.8 < K < 1.81 \quad & (K = 1.805 \text{ is used in Fig. 18(d)}), \end{aligned}$$

In these figures, N is the total number of points (iterations) plotted before the control is applied, and Nc is the number of points which have been affected by the corresponding control input.

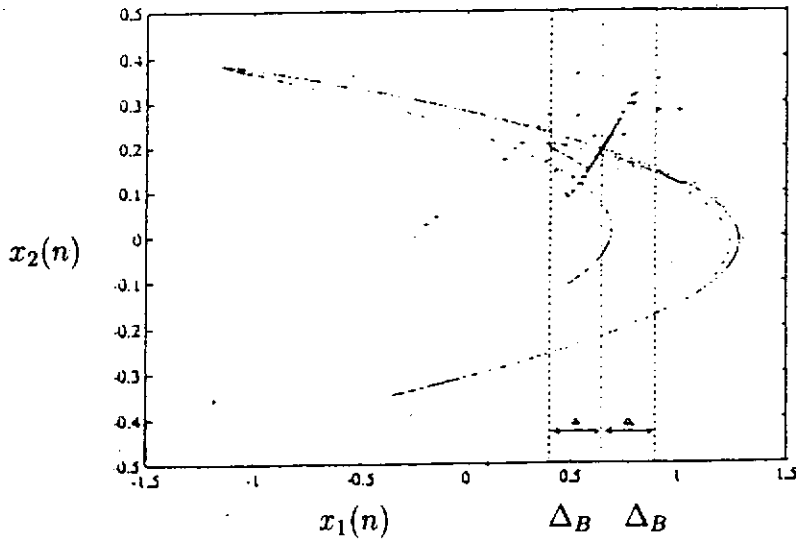

Fig. 19. Trajectory of the controlled Hénon system. $p = 1.3$, $q = 0.3$, $K = 0.9977$. (*Figure from Dong & Chen [1992a], courtesy of IEEE*; ©*1992 IEEE.*)

4.2.2. *Controlling the Hénon system*

Another interesting discrete-time chaotic system is the *Hénon* system:

$$\begin{cases} x_1(n+1) = -px_1^2(n) + x_2(n) + 1\,, \\ x_2(n+1) = qx_1(n)\,, \end{cases} \tag{30}$$

with real parameters p and q. It is known that the most significant (and unstable) one, $(\bar{x}_1, \bar{x}_2)$, of the two equilibrium points of the system is

$$\left(\frac{(q-1)+\sqrt{(q-1)^2+4p}}{2p},\, q\frac{(q-1)+\sqrt{(q-1)^2+4p}}{2p}\right). \tag{31}$$

Through the same procedure, one can verify that the range for the feedback gain K is given by the following:

$$\begin{cases} \max\{q-1-2p\bar{x}_1,\, q-1+2p\bar{x}_1\} < K < p^2(\bar{x}_1)^2+q\,, \\ -1 < p\bar{x}_1 < 1\,. \end{cases} \tag{32}$$

After numerous simulations, it was noticed [Dong & Chen, 1992a] that, for certain values of p and q, a direct application of feedback control using K calculated from Eq. (32) can drive the trajectory to reach the equilibrium point without trouble, provided that the control is applied after the system trajectory has entered the "basin" (a numerically determined region, defined by $|x_1(n) - \bar{x}_1| \leq \Delta_B < \infty$ for some constant $\Delta_B > 0$ and indicated by the two vertical lines in Fig. 19). In the figure, the control is applied after $n = N \geq 2000$ iterations *and* after the trajectory has entered the indicated region. In this particular figure, Nc is the number of trajectory points under the influence of control, with $N + Nc = 2500$. It can be seen from this figure that the controlled trajectory seems to be wandering for a short period of time right after the control input is applied, but very quickly it is driven to their target positions.

4.2.3. *Controlling continuous-time chaotic systems via feedback*

The general feedback approach just proposed is now applied to an example of continuous-time chaotic systems.

Consider again Duffing's equation [Eq. (2)] with $p = 1$ in the form

$$\begin{cases} \dot{x} = y\,, \\ \dot{y} = -p_2x - x^3 - p_1y + q\cos(\omega t)\,, \end{cases} \tag{33}$$

where we recall that p_1, p_2, q, and ω are systems parameters. Some typical periodic and chaotic solutions of Duffing's equation, when displayed in the x-y phase plane, are shown in Fig. 20, where $p_1 = 0.4$, $p_2 = -1.1$, $\omega = 1.8$, and (a) $q = 0.620$ (period 1), (b) $q = 1.498$ (period 2), (c) $q = 1.800$ (chaotic), (d) $q = 2.100$ (chaotic).

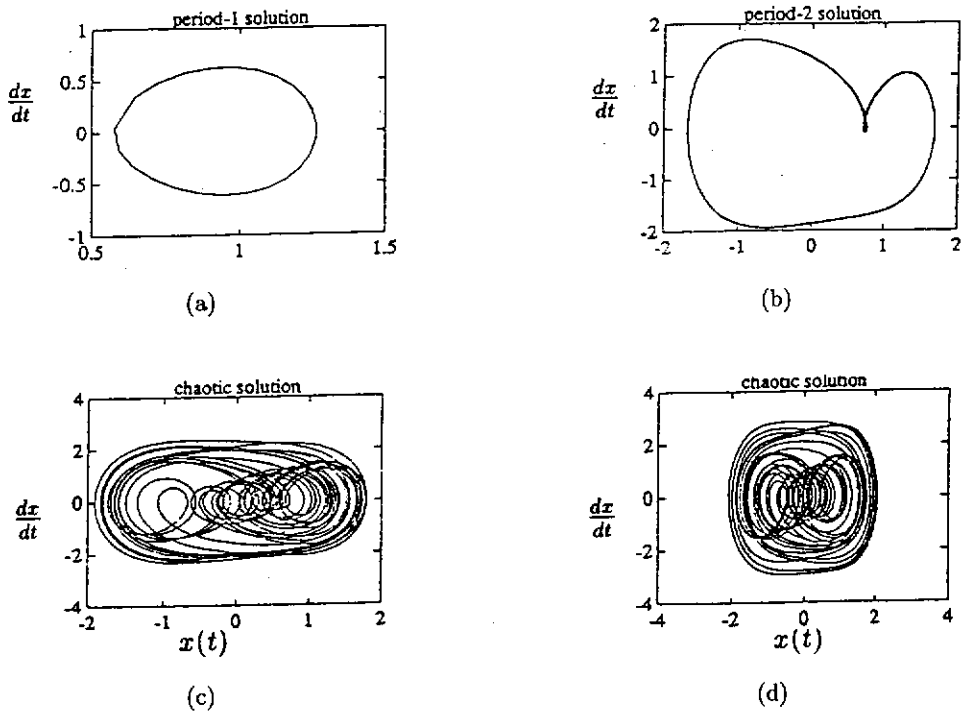

Fig. 20. Periodic and chaotic orbits of the Duffing system. (*Figure from Dong & Chen [1992b]*, courtesy of IEEE; ©*1992 IEEE.*)

As shown in the figures, with parameters $p_1 = 0.4$, $p_2 = -1.1$, $q = 2.1$, and $\omega = 1.8$, the Duffing system has a chaotic response.

For this system, one is interested in controlling the chaotic trajectories [e.g., those of Fig. 20(d)] when they appear, to one of the inherent unstable periodic orbits (limit cycles) of the system [e.g., that of Fig. 20(a) or Fig. 20(b)] by designing a conventional (preferably linear) feedback controller. In the above equation, let $(\bar{x}, \bar{y}) = (\bar{x}(t), \bar{y}(t))$ be the target, one of its periodic orbits. One wants to be able to control the system trajectory, so that for any given $\varepsilon > 0$ there exists a $T_\varepsilon > 0$ such that

$$|x(t) - \bar{x}(t)| \le \varepsilon \quad \text{and} \quad |y(t) - \bar{y}(t)| \le \varepsilon \quad \text{for all } t \ge T_\varepsilon . \tag{34}$$

For this purpose, consider the conventional nonlinear feedback controller of the form $u(t) = h(t; x, \bar{x})$, where h is a nonlinear function in general, which is added to the second equation of the original system. Then one obtains the following "controlled Duffing equation":

$$\begin{cases} \dot{x} = y , \\ \dot{y} = -p_2 x - x^3 - p_1 y + q\cos(\omega t) + h(t; x, \bar{x}) . \end{cases} \tag{35}$$

Observe that the periodic orbit $(\bar{x}, \bar{y})$ is itself a solution of the original equation. Subtracting Eq. (33), with (x, y) being replaced by $(\bar{x}, \bar{y})$ therein, from Eq. (35), and denoting $X = x - \bar{x}$ and $Y = y - \bar{y}$, one arrives at

$$\begin{cases} \dot{X} = Y - p_1 X , \\ \dot{Y} = -p_2 X - (x^3 - \bar{x}^3) + h(x) . \end{cases} \tag{36}$$

The design of the (nonlinear) feedback controller $h(x)$ will then be based on this model.

The following sufficient condition has been established by Chen [1993a]:

Theorem 1. *For any (stable or unstable) periodic solution $\bar{x}$ of Duffing's system, let the (feedback) control law be*

$$u(t) = -K[x(t) - \bar{x}(t)] + h(t; x, \bar{x}) \tag{37}$$

with $K \ge p_2$ and $h(t; x, \bar{x})$ satisfies

(i) $h(t; x, \bar{x}) - 3x\bar{x}(x - \bar{x}) \in L_1([t_1, \infty) \times S)$ *and*
(ii) $u \in L_1([t_1, \infty))$,

where S is the domain on which the system is defined. Then, starting from any point of the system trajectory at $t = t_1 \ge t_0$, the controlled trajectory of